Transonic Pressure Distributions on a Rectangular Supercritical Wing Oscillating in Pitch

Rodney H Ricketts,* Maynard C Sandford,†
David A Seidel,‡ and Judith J Watson§
NASA Langley Research Center, Hampton, Virginia

Steady and unsteady aerodynamic data were measured on a rectangular wing with a 12% thick supercritical airfoil mounted in the NASA Langley Transonic Dynamics Tunnel The wing was oscillated in pitch to generate the unsteady aerodynamic data The purpose of the wind tunnel test was to measure data for use in the development and assessment of transonic analytical codes The effects on the wing pressure distributions of Mach number, mean angle of attack, and oscillation frequency and amplitude were measured Results from the XTRAN3S program (a nonlinear transonic small disturbance code) and from the RHOIV program (a linear lifting surface kernel function code) were compared to data measured for a Mach number of 0 7 and for oscillation frequencies ranging from 0 to 20 Hz The XTRAN3S steady and unsteady results agreed fairly well with the measured data. The RHOIV unsteady result agreement was fair but, of course, did not predict shock effects

Nomenclature

b	= wing span, ft (4 0)
c	= wing chord, ft (2.0)
C_L	= total wing lift coefficient
C_p	= pressure coefficient, $(p-p_\infty)/q$
f	= wing pitch frequency, Hz
k	= reduced frequency, $c\omega/2V$
M	= freestream Mach number
p	= transducer local static pressure, lb/in ^{2}
p_∞	= freestream static pressure, lb/in.^{2}
q	= freestream dynamic pressure, lb/in.^{2}
t/c	= thickness to chord ratio
V	= freestream velocity, ft/s
x/c	= fractional chord
α	= mean angle of attack, deg
$\Delta\alpha$	= pitch oscillation amplitude, deg
ΔC_p	= lifting pressure coefficient (difference between lower- and upper-pressure coefficients)
$\lvert\Delta C_p\rvert$	= magnitude of lifting pressure coefficient
η	= fractional span, y/b
ϕ	= phase between lifting pressure and wing pitch angle, deg (positive for pressure leading motion)
ω	= circular frequency, rad/s

Introduction

IN recent years NASA Langley Research Center has had a program for measuring unsteady aerodynamic data in the transonic regime for the purposes of assisting analytical code development and providing a data base for active controls design Two models previously tested in the 16-ft Transonic Dynamics Tunnel (TDT) are a clipped delta wing[1] and a high aspect ratio transport wing.[2] The delta wing, which has a circular arc airfoil, was oscillated in pitch at various mean angles of attack A trailing edge control also was oscillated to generate unsteady aerodynamic data The transport type wing with a supercritical airfoil has five leading edge and five trailing-edge control surfaces, some of which were oscillated independently and in pairs about various mean control surface angles The static angle of attack of the transport-type was varied to allow data acquisition at cruise lift conditions

Wind-tunnel tests have been completed on a third wing—a rectangular wing having a supercritical airfoil This particular wing (having a simple planform geometry) was tested for the purpose of aiding in the development and preliminary assessment of new analytical transonic codes such as XTRAN3S (Refs 3 and 4). The results obtained from this test provide the database desired for extension of two dimensional flows to three-dimensional flows The present paper describes this recent test of the rectangular wing, presents measured data, and correlates these experimental results with theoretical results

Wing Configuration

A photograph of the wing installed in the TDT is shown in Fig 1 The wing is attached to a shaft that extends through a

Fig. 1 Wing mounted in TDT test section

Received March 12 1983; presented as Paper 83 0923 at the 24th AIAA/ASME/ASCE/AHS Structures Structural Dynamics and Materials Conference Lake Tahoe Nev May 2 4 1983; revision received Jan 12 1984 This paper is declared a work of the U S Government and therefore is in the public domain

*Leader Aircraft Aeroelasticity Group Configuration Aeroelasticity Branch Member AIAA

†Aero-Space Technologist, Configuration Aeroelasticity Branch Member AIAA

‡Aero Space Technologist Unsteady Aerodynamics Branch. Member AIAA

§Aero Space Technologist Structural Concepts Branch Member AIAA

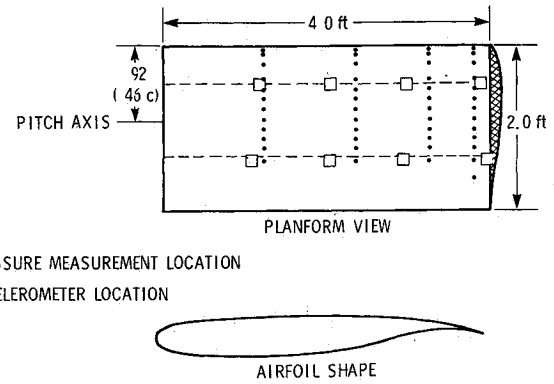

Fig 2 Planform view and airfoil shape of wing (dimensions in ft)

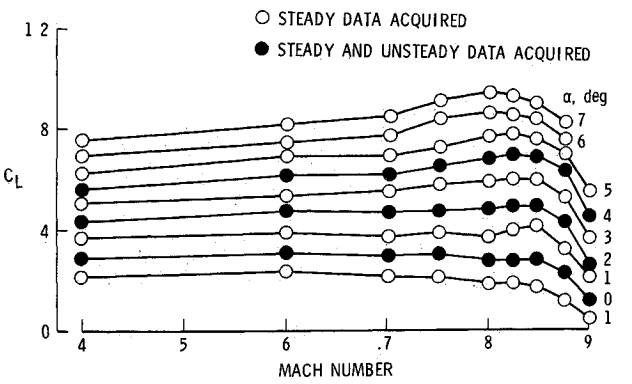

Fig 3 Total wing lift coefficient for various angles of attack plotted against Mach number

splitter plate mounted off the wind-tunnel wall so that the wing root is outside the wall boundary layer The shaft is connected to a hydraulic rotary actuator that oscillates the wing in pitch.

The planform and airfoil shape are shown in Fig. 2 The unswept wing has a rectangular planform with a 2 ft chord and a 4-ft span (panel aspect ratio of 2 0) The airfoil is a 12% thick ($t/c = 0$ 12) supercritical shape with a two dimensional design Mach number of 0 8 and design lift coefficient of 0 6 This airfoil was chosen as being typical of those being em ployed on new transport aircraft The wing tip was formed by connecting the upper and lower surfaces with semicircular arcs The wing pitch axis is located at the 0 46 fractional chord Details of the geometric properties, including the airfoil coordinates, and the structural properties of the wing are presented in Ref 5.

Instrumentation

Wing instrumentation consisted of 126 differential pressure transducers, eight accelerometers, and one potentiometer The transducers were mounted at four spanwise stations to measure both static and dynamic pressures along chordwise rows (see Fig. 2) on the upper and lower surfaces Both in situ transducers and transducers utilizing the Dutch matched tubing technique[6] were mounted in the wing Each transducer was referenced to the tunnel static pressure The poten tiometer and accelerometers were used to measure static and dynamic motions of the wing Details of the instrumentation are presented in Ref 5

Wind Tunnel

The Langley Transonic Dynamics Tunnel (TDT) is a closed circuit continous flow tunnel which has a 16 ft square test section with cropped corners and slots in all four walls Mach number and dynamic pressure can be varied simultaneously, or independently, with either air or Freon¶ used as a test medium. All data presented in this report were obtained using a Freon medium

Data Acquisition and Reduction

Data from the model instrumentation were acquired using the TDT real time data acquisition system [7] Steady (static) pressures were measured using the differential pressure transducers installed in the wing One thousand samples of data at a rate of 300 samples/s were averaged for each transducer to determine mean values of pressure coefficient Unsteady (dynamic) pressures were calculated from trans ducer time history data measured at a rate of 300 samples/s and recorded on digital tape A discrete Fourier transform of

¶Freon is a registered trademark of E I DuPont de Nemours & Co Inc Use of trade names does not constitute an official en dorsement either expressed or implied by NASA

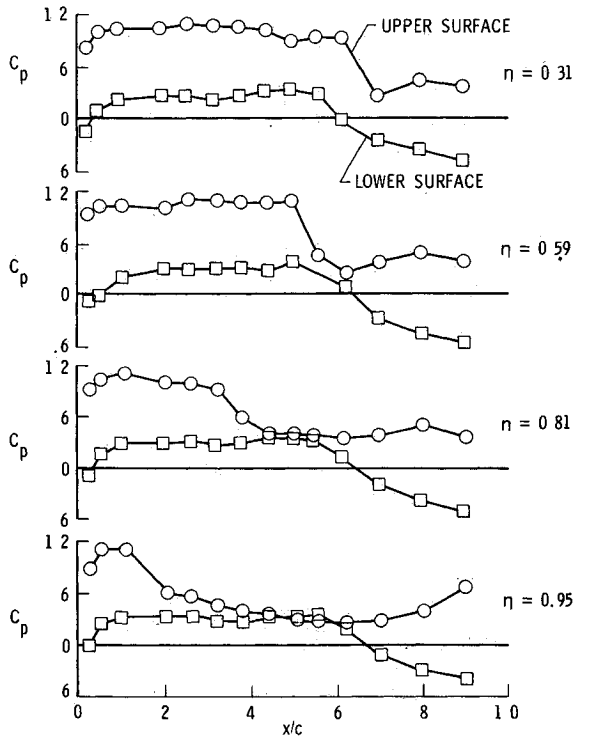

Fig 4 Steady pressure distributions at four spanwise stations; $M = 0$ 825, $\alpha = 4$ deg

75 100 cycles of the data (a minimum of 15 samples/cycle) was used to determine the first harmonic pressure coefficient magnitude and phase in relation to the pitch position of the wing root The magnitude and phase measurements from transducers using the matched-tubing method were deter mined using transfer functions derived from calibration data from corresponding in situ and matched tubing transducers.

Test Results and Discussion

As illustrated in Fig 3, steady and unsteady pressures were measured[8] for a large number of test conditions in the TDT The figure shows the wing total lift coefficient plotted against Mach number for angles of attack ranging from −1 to 7 deg For the unsteady data points (solid symbols) in Fig 3, the wing oscillation frequencies were 5, 10, 15, and 20 Hz Some representative results obtained during these tests are presented. The Reynolds number based on the chord length is four million for all data presented

Steady Results

Upper and lower-surface steady pressure distributions at the four spanwise stations are shown in Fig 4 for a Mach

number of 0 825 and an angle of attack of 4 deg (This is close to the two dimensional design condition for the airfoil) At the inboard sections, typical supercritical flow is present on the upper surface, that is, there is a rather flat pressure region followed by a weak shock far aft (0 50 to 0 60 fractional chord) on the wing However, for sections farther out on the wing, this shock is farther forward toward the leading edge as a result of the effects of the wing tip At the wing tip the shock is located at about the 0 10 fractional chord The pressure distributions on the lower surface are not affected by the presence of the wing tip

Unsteady Results

Some of the unsteady pressure distributions measured during the tests are summarized in this section The results are presented in terms of the magnitude and phase of the lifting pressure coefficient ($|\Delta C_p|$ and ϕ, respectively) In the figures presented in this section, curves are faired through the data points in the region of the shock to show trends and estimated peak-pressure (shock) locations

Span Effects

Pressure distributions at the four spanwise stations are shown in Fig. 5 for a mean angle of attack of 4 deg and a Mach number of 0 825. The oscillation amplitude and frequency are ±1 deg and 10 Hz ($k=0$ 15), respectively The pressure peaks, which are indicative of dynamic shock motion, vary significantly across the wing span By com parison with the steady data (Fig 4), it is observed that the pressure peaks are located near the same chordwise positions as the upper surface static shocks The unsteady shock strength decreases nearer the tip region The phase results in Fig 5 show that the pressure is generally lagging the wing pitch motion (negative phase) forward of the pitch axis (0.46 fractional chord) and leading it aft of the axis For the two inboard stations where the shocks are located aft of the pitch axis, the lag-to-lead phase shift occurs aft of the shock

Mach Number Effects

Pressure distributions at the inboard station (0.31 fractional span) are shown in Fig 6 for seven Mach numbers ranging from 0 4 to 0.85 The wing mean angle of attack is 2 deg The oscillation amplitude and frequency are ±1 deg and 10 Hz, respectively (k ranges from 0 31 at 0 4 Mach number to 0 15 at 0 85 Mach number) The pressure peak is located at the leading edge for the low subsonic Mach numbers but rapidly moves aft as the Mach number increases At a Mach number of 0 85 the estimated shock location is near the three quarter chord This is better shown in Fig 7 where the estimated shock location in fractional chord is shown plotted against Mach number In this figure it is seen that the shock begins to move aft rapidly as the Mach number is increased above 0 6 For the most part, the phase data (see Fig 6) show that the pressures lag the motion ahead of the shock and lead behind the shock

Mean Angle of-Attack Effects

Pressure distributions at the inboard station (0 31 fractional span) are shown in Fig 8 for three mean angles of attack at a Mach number of 0 825 The oscillation amplitude and frequency are ±1 deg and 10 Hz ($k=0$ 15), respectively The results show that, as the angle of attack increases, the shock moves aft on the wing, and the pressures ahead of the shock decrease considerably in magnitude The phase data show that the pressures lag the motion ahead of the shock and lead the motion aft of the shock For increasing mean angles of attack, the phase angles ahead of the shock increase slightly

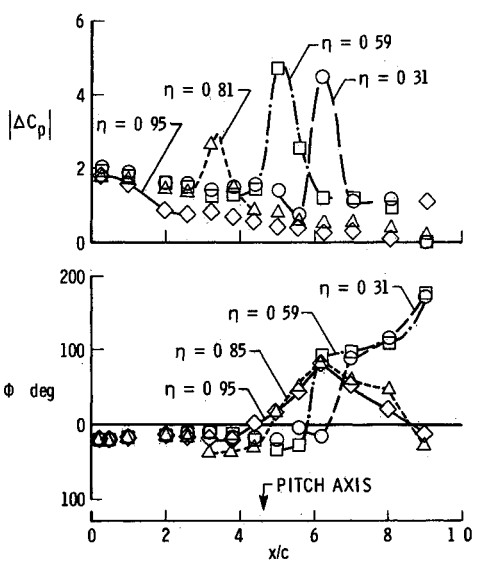

Fig 5 Effects of span on unsteady pressure distributions at four spanwise stations; $M=0.825$, $\alpha=4$ deg, $f=10$ Hz, $\Delta\alpha=\pm$ deg

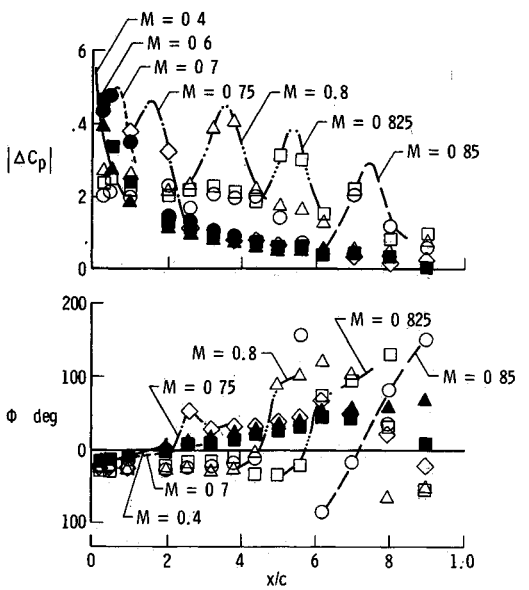

Fig 6 Effects of Mach number on unsteady pressure distribution at $\eta=0$ 31; $\alpha=2$ deg, $f=10$ Hz, $\Delta\alpha=\pm1$ deg

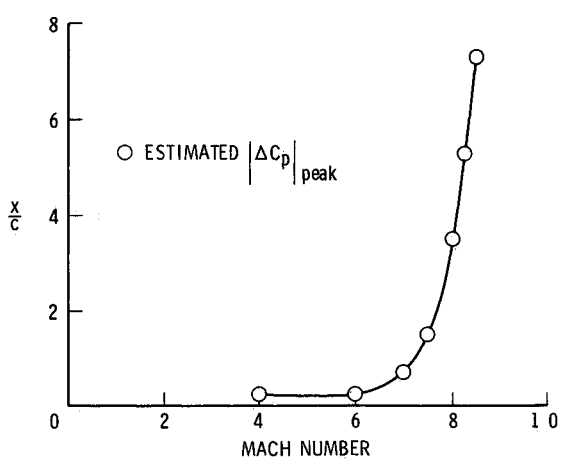

Fig 7 Effect of Mach number on estimated shock location in fractional chord; $\alpha=2$ deg, $f=10$ Hz, $\Delta\alpha=\pm1$ deg

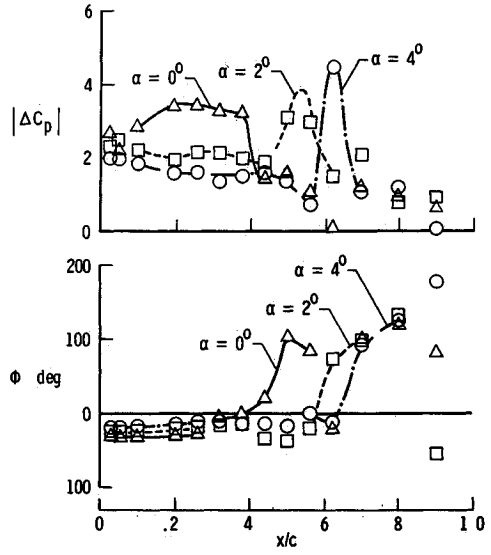

Fig. 8 Effects of mean angle of attack on unsteady pressure distribution at $\eta = 0.31$; $M = 0\ 825$, $f = 10$ Hz, $\Delta\alpha = \pm$ deg

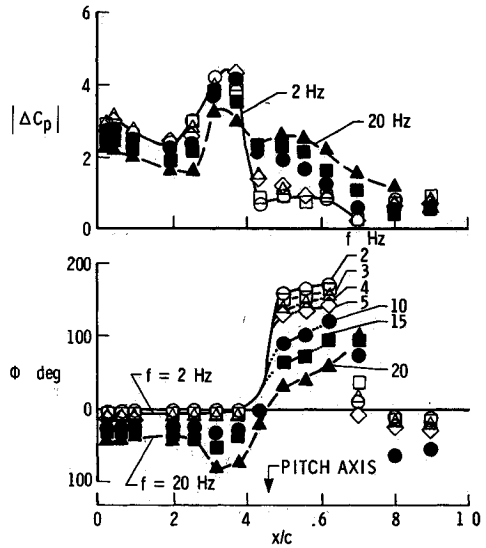

Fig 9 Effects of frequency on unsteady pressure distribution at $\eta = 0.31$; $M = 0\ 8$, $\alpha = 2$ deg, $\Delta\alpha = \pm 1$ deg.

Oscillation Frequency Effects

Pressure distributions at the inboard chord (0 31 fractional span) are shown in Fig 9 for seven oscillation frequencies ranging from 2 to 20 Hz ($k = 0.03$ to 0 31) and an oscillation amplitude of ± 1 deg. The Mach number and mean angle of attack are 0 8 and 2 deg, respectively The results show that the frequency effect is large for both the magnitude and phase As the frequency of oscillation increases, the magnitude of the pressure generally decreases forward of the pitch axis and increases behind the axis The shock at ap proximately the 0 35 fractional chord coincides with the steady-state shock location and appears to decrease in strength as the frequency increases. The phase results show that the pressures lag the motion ahead of the shock and lead the motion behind the shock The phase angle generally decreases (pressure lags the motion) as the frequency increases This effect is more pronounced aft of the pitch axis

Oscillation Amplitude Effects

Pressure distributions for the inboard chord (0 31 fractional span) are shown in Fig. 10 for three oscillation amplitudes ranging from 0 5 to 1 5 deg and an oscillation frequency of 10 Hz ($k = 0.16$). The Mach number and mean

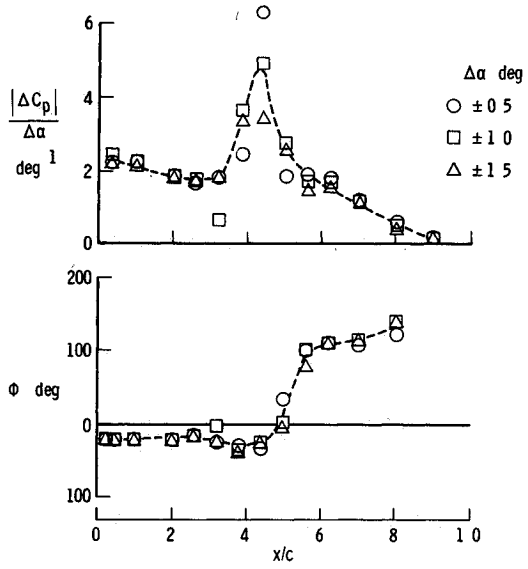

Fig 10 Effects of oscillation amplitude on unsteady pressure distribution at $\eta = 0\ 31$; $M = 0\ 8$, $\alpha = 3\ 3$ deg, $f = 10$ Hz

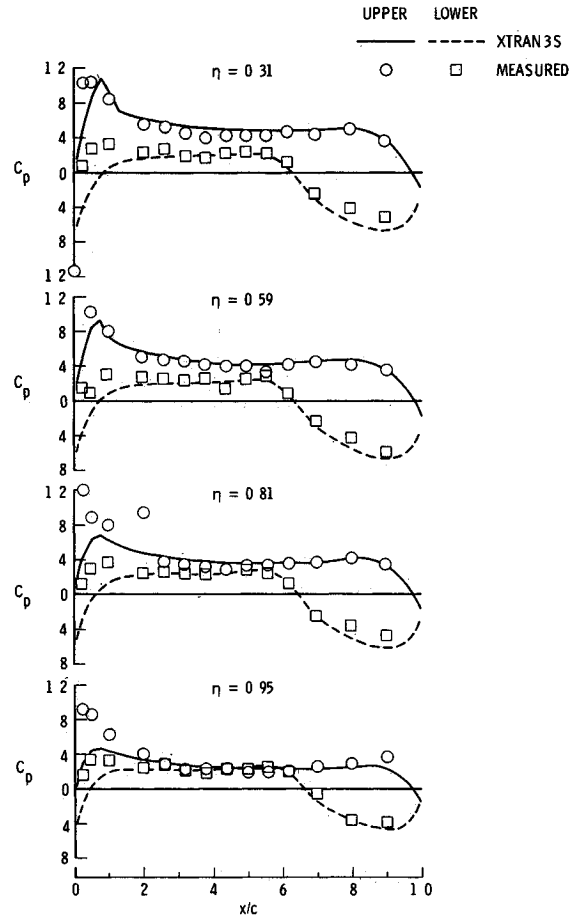

Fig 11 Spanwise comparison of measured and calculated steady pressure distributions; $M = 0\ 7$, $\alpha = 2$ deg

angle of attack are 0 8 and 3 3 deg, respectively In the figure the pressure magnitudes are normalized by the oscillation amplitudes and show no appreciable difference either forward or aft of the shock for the three cases Therefore, in these regions it follows that the pressure magnitude increases linearly as the motion amplitude is increased in the range 0 5 to 1 5 deg. In the vicinity of the pressure peak there are differences in data which indicate magnitude nonlinearities in

this region. No effect of oscillation amplitude is seen in the pressure phase data.

Comparison of Measured and Calculated Results

Unsteady pressure calculations were made with two theoretical programs, and the results are compared with measured data. One program is XTRAN3S, (Refs. 3 and 4), a three-dimensional nonlinear transonic code using finite difference methods to approximate a time-accurate solution from the small disturbance potential equation. The version of the code used does not include the effects of viscosity. In order to improve accuracy and agreement with measured data, the XTRAN3S results made use of 1) a revised grid arrangement,[9,10] and 2) small-disturbance equation coefficients derived by the National Aerospace Laboratory of the Netherlands.[11] The other program used for the unsteady pressure comparisons is RHOIV[12], a linear subsonic lifting surface kernel function theory based on the acceleration potential. In addition to the unsteady comparisons, steady pressure comparisons are made using the XTRAN3S program.

Comparisons are made for calculated and measured results at a Mach number of 0.7. The mean angle of attack is 2 deg. The oscillating amplitude and frequency range for the unsteady data are ± 1 deg and 5 to 20 Hz ($k=0.09$ to 0.36), respectively. Rigid pitch motions were used in the unsteady calculations. For XTRAN3S results, the measured wing coordinates were used.

Steady Results

Comparisons of steady upper- and lower-surface pressure distributions at the four span stations are shown in Fig. 11. The comparisons are good over most of the wing. At all spanwise stations the XTRAN3S program accurately predicted both the upper-surface pressures aft of the shock and the lower-surface pressures in the midchord region. The results deviate somewhat in the leading-edge region and on the lower surface near the trailing edge. The comparisons in these regions may possibly be improved by including viscous effects in the code and by decreasing the grid spacing for the calculations in this region to account for the bluntness of this

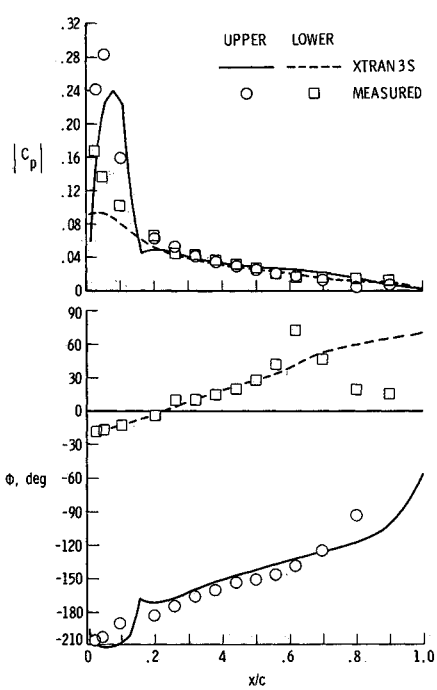

Fig. 12 Comparison of measured and calculated first harmonic unsteady pressure distribution at $\eta=0.59$; $M=0.7$, $\alpha=2$ deg, $f=10$ Hz, $\Delta\alpha=\pm 1$ deg.

airfoil (see Fig. 2). Analysis (not shown) of this airfoil with the two-dimensional full potential program[13] indicated that including viscous effects at this condition tends to raise the lower-surface pressures in the leading-edge region as a result of a decambering effect of the boundary layer in the aft portion of the airfoil. A finer grid may improve the upper-surface pressure-peak definition near the leading edge.

Calculations for a Mach number of 0.825 (not shown here) showed significantly poorer agreement than the results for 0.7 Mach number. For this case the upper-surface shock was calculated to be near the trailing edge rather than located as shown in Fig. 4. Again, the two-dimensional program indicated that inclusion of viscosity in the solution causes the shock to move forward nearer its proper location (approximately 0.6 fractional chord at the inboard spanwise station).

Unsteady Results

Upper- and Lower-Surface Pressure Comparison

Unsteady upper- and lower-surface pressure distributions from measurements and XTRAN3S calculations are shown in Fig. 12 at a fractional span of 0.59 and an oscillation amplitude and frequency of ± 1 deg and 10 Hz ($k=0.18$), respectively. The agreement of the pressure magnitudes is good over the aft three-quarters of the chord for both the upper- and lower- surface data. In the leading-edge region near the shock, the agreement is not as good. In this region XTRAN3S underestimated the magnitudes. The phase agreement is good over the forward three-quarters of the chord and degrades significantly near the trailing edge. No explanation for this disagreement is apparent.

Spanwise Pressure Comparison

Unsteady lifting pressure distributions at the four spanwise stations are shown in Fig. 13. The comparison includes both measured data and results from XTRAN3S and RHOIV The XTRAN3S program predicted fairly well the pressure magnitudes at all spanwise stations in the region aft of the shock (located near the leading edge). In the region of the shock the calculations overestimated the leading-edge pressures at the inboard station and underestimated those pressures at the outboard stations. The phase agreement is good over the forward half of the chord at the outboard three stations. The phase calculations at the most inboard station are affected by the overestimated leading-edge shock and are not in good agreement with measured values. The phase agreement is also not good near the trailing edge at all span stations. In this region the measured lifting-pressure phases show a strong influence of the lower-surface-pressure phase (see Fig. 12). The RHOIV results are presented for 0.31, 0.59, and 0.81 fractional span stations. The pressure-magnitude agreement is fairly good over the aft two-thirds of the chord. However, at all spanwise stations the magnitude is underestimated in the forward half of the wing and overestimated in the aft portion of the wing. The leading-edge shock, of course, is not predicted by the linear theory. The phase agreement is good over the forward two-thirds of the wing and, in most cases, is better than the XTRAN3S agreement. As with the XTRAN3S results, the phase agreement near the trailing edge is not good.

Frequency Comparison

Unsteady lifting pressure distributions at a fractional span of 0.59 are shown in Fig. 14 for oscillation frequencies of 5, 10, 15, and 20 Hz ($k=0.09$ to 0.36). The comparison includes measured data and results from both XTRAN3S and RHOIV. In general, the XTRAN3S agreement is fairly good for the phase and magnitude data. For these cases the strength of the shock at the leading edge is best predicted at the lowest frequency. At higher frequencies the shock strength is underestimated. The phase agreement is best at the two higher

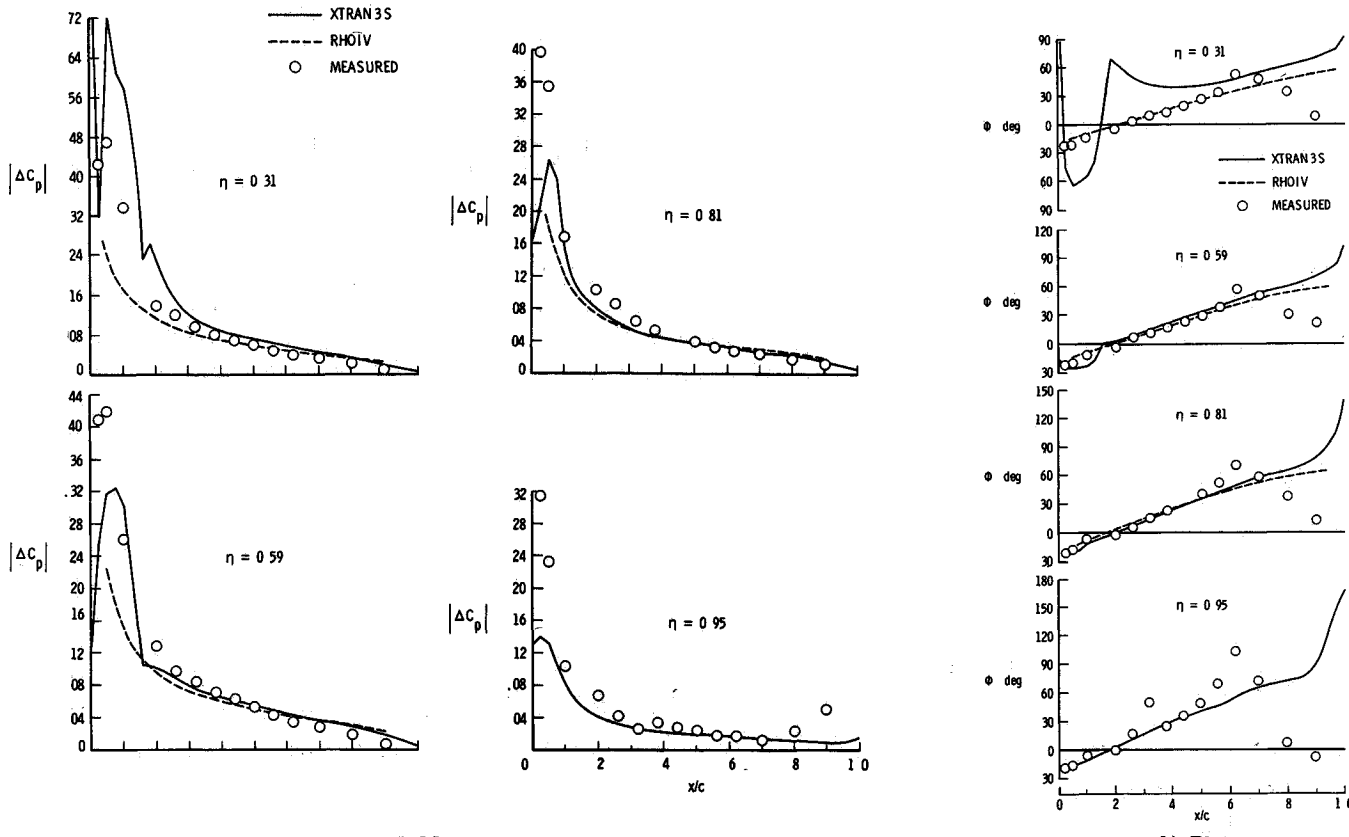

a) Magnitude b) Phase

Fig 13 Spanwise comparison of measured and calculated unsteady pressure distributed; $M=0.7$, $\alpha=2$ deg, $f=10$ Hz, $\Delta\alpha=\pm1$ deg

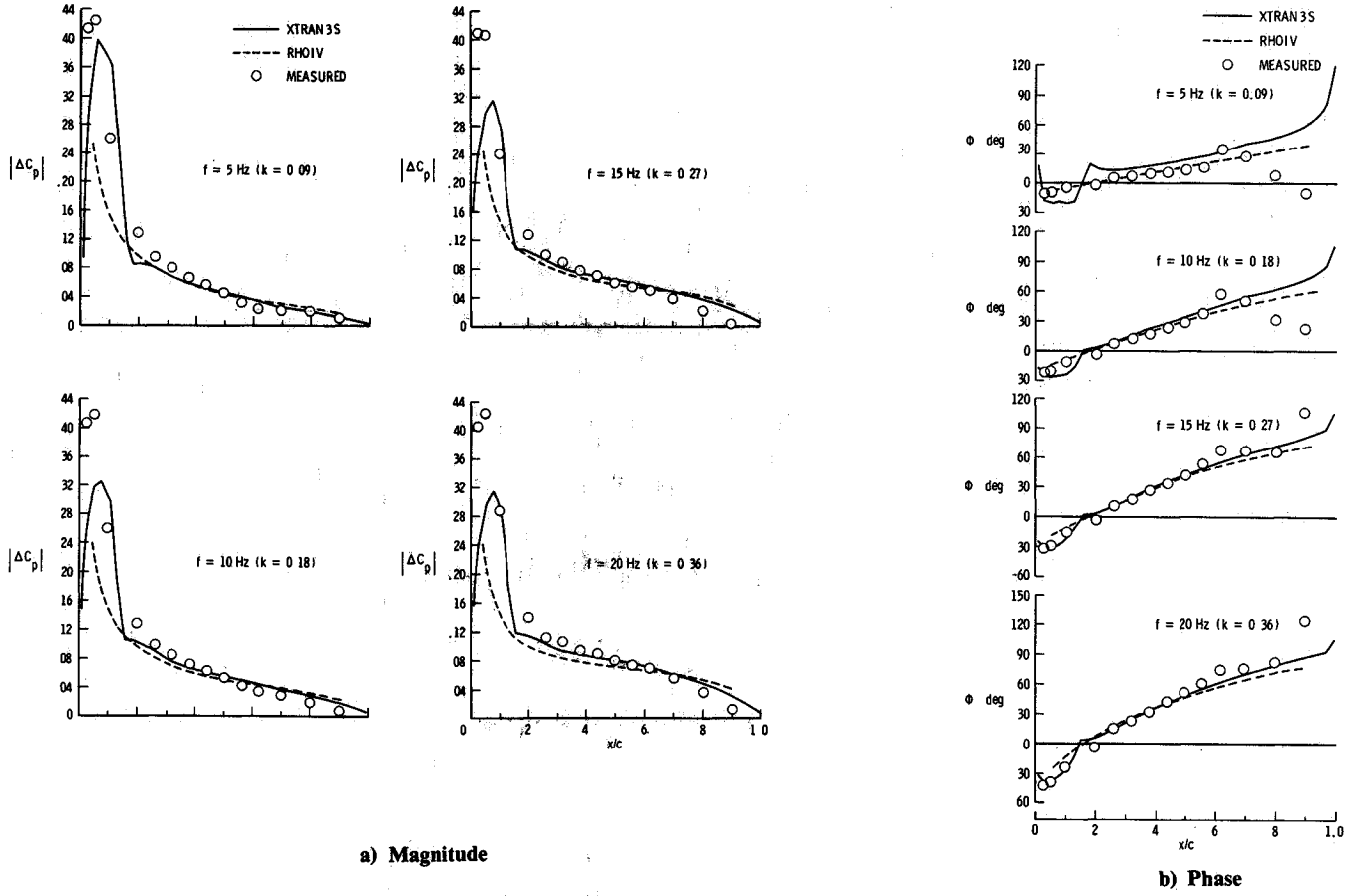

a) Magnitude b) Phase

Fig 14 Effect-of-frequency comparison at $\eta=0.59$; $M=0.7$, $\alpha=2$ deg, $\Delta\alpha=\pm1$ deg.

frequencies where the measured data do not have the monotonically increasing trend reversed near the trailing edge The RHOIV magnitude agreement is fairly good in the aft two-thirds of the chord at all frequencies. The phase agreement in the forward two-thirds of the chord is good and improves as the frequency decreases

Summary

Both steady and unsteady aeroynamic data were measured on a rectangular wing with a 12% thick supercritical airfoil The wing was oscillated in pitch to acquire the unsteady data The purpose of the test was to provide experimental data to assist in the development and assessment of transonic analytical codes The effect of the wing tip (that is, three dimensional effects) on the pressure distributions is large Specifically, the shock location at the outboard sections is considerably farther forward than for inboard sections Parameters that also have a large effect on the shock strength and location include Mach number and mean angle of attack Oscillation frequency has a significant effect on the unsteady-pressure magnitudes and phases Oscillation amplitude affects the unsteady pressure magnitudes in a linear manner, except at the shock where some nonlinearity exists

Results from the XTRAN3S nonlinear transonic programs and from the linear RHOIV kernel function program were compared to the measured data. The XTRAN3S steady and unsteady results agreed fairly well with measured data at a Mach number of 0 7. It is believed that the inclusion of viscosity in the analysis and use of a finer grid will give better results, particularly at the wing leading edge The RHOIV unsteady results were in fair agreement, but, of course, the location or strength of the shock was not predicted

References

[1]Hess R. W. Wynne, E C , and Cazier F W Jr Static and Unsteady Pressure Measurements on a 50 Degree Clipped Delta Wing at M=0 9 " AIAA Paper 82 0686 (also available as NASA TM 83297 April 1982)

[2]Sandford M C Ricketts, R H , Cazier F W Jr , and Cun ningham H J 'Transonic Unsteady Airloads on an Energy Ef ficient Transport Wing with Oscillating Control Surfaces *Journal of Aircraft* Vol 18, July 1981 pp 557 561

[3]Borland C J and Rizzetta, D P , ' Nonlinear Transonic Flutter Analysis " AIAA Paper 81 0608 April 1981

[4]Borland, C J and Rizzetta, D P 'Transonic Unsteady Aerodynamics for Aeroelastic Applications—Technical Development Summary " AFFWAL TR 80 3107, Vol 1 June 1982

[5]Ricketts, R H , Watson J J Sandford M C and Seidel D A "Geometric and Structural Properties of a Rectangular Super critical Wing Oscillated in Pitch for Measurement of Unsteady Transonic Pressure Distributions ' NASA TM 85673, Nov 1983

[6]Tijdeman, H , Investigations of the Transonic Flow Around Oscillating Airfoils, ' National Aerospace Laboratory, Amsterdam NLRTR 77090 U 1977 (available from DTIC as AD B027 633)

[7]Cole, P H , "Wind Tunnel Real Time Data Acquisition System," NASA TM 80081, April 1979

[8]Ricketts R H Sandford, M C Watson J J and Seidel D A Subsonic and Transonic Unsteady- and Steady Pressure Measurements on a Rectangular Supercritical Wing Oscillated in Pitch," NASA TM 85765 July 1984

[9]Seidel D A Bennett, R M and Whitlow, W Jr. ' An Ex ploratory Study of Finite Difference Grids for Transonic Unsteady Aerodynamics " AIAA Paper 83 0503 (also available as NASA TM 84583 Dec 1982)

[10]Seidel, D A , Bennett, R M and Ricketts R H , "Some Recent Applications of XTRAN3S," AIAA Paper 83 1811 (also available as NASA TM 85641 May 1983)

[11]Van der Vooren J , Sloof, J W., Hizing, G H and Van Essen A , Remarks on the Suitability of Various Transonic Perturbation Equations to Describe Three Dimensional Transonic Flow—Examples of Computations Using a Fully Conservative Rotated Difference Scheme,' *Proceedings of Symposium Tran sonicum II* Springer Verlag, Berlin 1976 pp 557 566

[12]Redman M C and Rowe, W S , ' Prediction of Unsteady Aerodynamic Loadings Caused by Leading Edge and Trailing Edge Control Surface Motions in Subsonic Compressible Flow—Computer Program Description ' NASA CR 132634 1975

[13]Bauer F , Garabedian P Korn D and Jameson A , *Supercritical Wing Sections II: Lecture Notes in Economics and Mathematical Systems* edited by M Beckmann and H P Lunzi Springer Verlag 1975